Lung Lesion Images Classification Based on Deep Learning Model and Adaboost Techniques

Nguyen Thanh Binh[1,2(✉)] and Vuong Bao Thy[3]

[1] Department of Information Systems, Faculty of Computer Science and Engineering, Ho Chi Minh City University of Technology (HCMUT), VNU-HCM 268 Ly Thuong Kiet Street, District 10, Ho Chi Minh City, Vietnam
ntbinh@hcmut.edu.vn

[2] Vietnam National University Ho Chi Minh City, Linh Trung Ward Thu Duc City, Ho Chi Minh City, Vietnam

[3] Faculty of Health Sciences, University of Cuu Long, Vinh Long, Vietnam
vuongbaothy@mku.edu.vn

Abstract. Today, the medical industry is promoting the research and application of artificial intelligence in disease diagnosis and treatment. The development of diagnostic methods with the support of electronic devices and information technology can help doctors save time in diagnosing and treating diseases, especially medical images. Diagnosis of lung lesions based on lung images is a case study. This paper proposed a method for lung lesion images classification based on modified U-Net and VGG-19 combined on adaboost techniques. The modified U-Net architecture with 5 pooling and 5 unpooling. It has the unpooling layer with kernels of size 2×2, stride 2×2 to get output consistent with the adaboost. The result of the proposed method is about 97.61% and better results than others in the Covid-19 radiography dataset.

Keywords: Classification · U-Net · Lung lesion images · VGG-19 · Adaboost

1 Introduction

The application of science and technology to the field of health science has been promoted in recent years, especially the application of intelligent processing technology, artificial intelligence to disease diagnosis and treatment. Specifically, the application stages include prediction, screening, analysis and decoding medical image data containing abnormalities.

Covid-19 has been spreading rapidly since the end of 2019. Early detection of people infected with Sars-Cov-2 for treatment is urgent work today. Because infecting subjects that are not detected in time will spread the virus to others [1, 2]. Testing by RT-PCR method is considered as the key to detect Sars-Cov-2 virus [3]. However, this method is time consuming and sometimes test results are misleading.

C. V. Phan and T. D. Nguyen (Eds.): ICCASA 2022, LNICST 475, pp. 102–111, 2023.
https://doi.org/10.1007/978-3-031-28816-6_8

Imaging techniques, such as chest X-ray and chest CT, have been widely used to evaluate lung lesions. Although the X-Ray scanner showed a higher accessibility, most of the Sars-Cov-2 infected subjects showed a bilaterally blurred parenchymal background and the lung shape fused into a circular morphology [6], making it difficult to distinguish Sars-Cov-2 infection when viewing radiographs. In contrast, 3D chest CT is effective in soft tissue differentiation and morphological imaging of lung parenchyma. This image has been widely used for the diagnosis of Covid-19 and is considered an important adjunct to RT-PCR tests [3–5]. Medical image processing using deep learning plays an important role due to its high accuracy and efficiency [7]. The deep learning-based approach has proven highly accurate in detecting Covid-19.

Li [8] used 2D U-Net to segment the lung ROI on CT slices, and then developed COV-Net incorporating ResNet-50 as the backbone to perform Covid-19 detection. Objects are extracted locally from each slice, and an aggregate layer is used to detect global features from a set of local features. The [9] proposed method to improve the CNNs for lung diseases image classification to detect pneumonia images. Javaheri [10] proposes the CovidCTNet method, which uses BCDU-Net for lung segmentation and a convolutional neural network (CNN) to distinguish Covid-19 from other pneumonia. BCDU-Net was pre-trained using data from a Kaggle lung segmentation contest [11].

Prasad [12] used U-Net with ResNet-50 pre-learned weights to detect Covid-19 infection. Hien [13] proposed a method using fuzzy C means for edge detection. Hemdan [14] proposed a method to diagnose Covid-19 by the COVIDX-Net model consisting of seven convolutional neural networks (CNNs). Chest X-ray images and breast cancer diagnosis on mammograms. Although those studies have yielded many good results. However, at present, the research results have the disadvantage that the proposed method is complicated, and the accuracy is not high. To overcome the above drawback, we propose a method of applying deep learning networks to classify images containing lung lesions of patients infected with Sars-Cov-2 virus with high accuracy and comparable with other methods of recently available legislation.

This paper proposed a method for lung lesion images classification based on modified U-net and VGG-19 combined on adaboost techniques. Main contributions of this study are: (i) the types of lung lesions are explained; (ii) proposed a method for lung lesion images classification based on deep learning model combined on adaboost techniques traditionally but with high accuracy results. The rest of the paper is organized as follows: Sect. 2 presents the U-net architectures, VGG-19 architectures, and the proposed method for classification. Section 3 and 4 are the experimental results and conclusions, respectively.

2 Lung Lesion Images Classification Based on Modify U-Net and VGG-19 Combined on Adaboost Techniques

2.1 U-Net and VGG-19 Architectures

The U-Net network consists of two main parts similar to the auto encoder model such as: encoder and decoder. However, they have an additional skip connection (similar to ResNet's) between layers and have the same size in the encoder – decoder. Since in

image translation, there is a lot of low-level information that needs to be shared between input and output, passing the information across these networks is necessary. It provides sufficient information to limit the loss of information during feature extraction [15].

U-Net architecture also reduces the phenomenon of vanishing derivatives when training. This phenomenon occurs when the derivative of the error function is too small and approaches 0. Therefore, it is almost impossible for the model to update the parameters based on the derivative of the error function, leading to the model not being able to converge. This phenomenon appears quite commonly in CNN models. Thanks to skip-connection, U-Net has overcome the above phenomenon during training, making it more efficient to update the derivative parameter of the error function. Because it is possible to update the derivative parameter of the error function more efficiently and avoid data loss at the feature extraction stage, U-Net can still ensure high accuracy without too much data training.

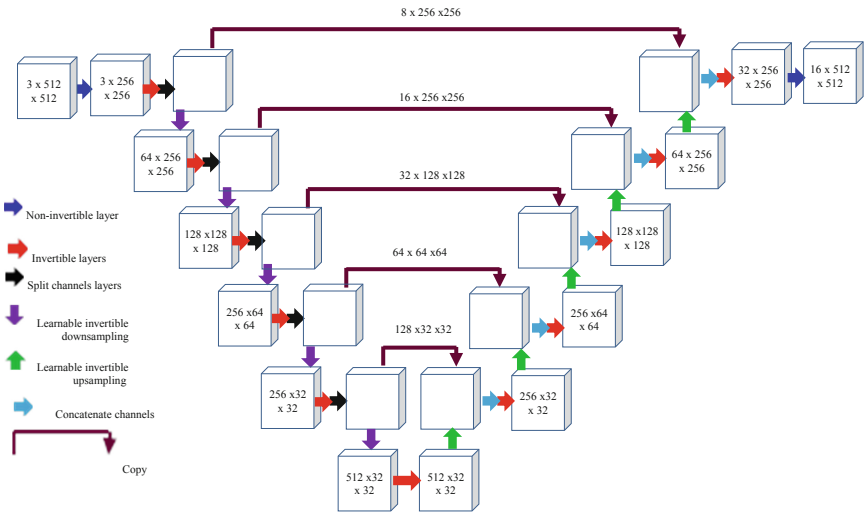

Fig. 1. The MoU-Net architecture [15]

The structure of the U-Net network: the first half of the U-Net network is a CNN consisting of convolutional, ReLU, and pooling network layers. The size of each layer gradually changes after each pooling. The first half of U-Net extracted features in the image. The second half of U-Net has the same structure as the first half of the network. However, the pooling layers are replaced by inverse convolution layers which increase the size of the layers to restore the features of the previously extracted image.

With the advantage of preserving information, avoiding the phenomenon of disappearing derivatives when training, the system uses U-Net as the generating network in the anomaly detection mode. The size of lung lesions is very small. So, we need to modify the U-Net architecture. We use the encoding path to extract low-level features and the decoding path to extract high-level features [15]. The Fig. 1 presented the modifying U-Net architecture (MoU-Net).

VGG is a convolutional neural network (CNN) architecture which helps to increase the depth of such networks. The only other component being pooling layers and a fully connected layer. The network uses small 3 x 3 filters. VGG-19 used 3 $\times$ 3 convolutional layers stacked and alternated with max pooling. It has two 4096 fully-connected layers and a softmax classifier. The VGG-19 architecture is present as Fig. 2.

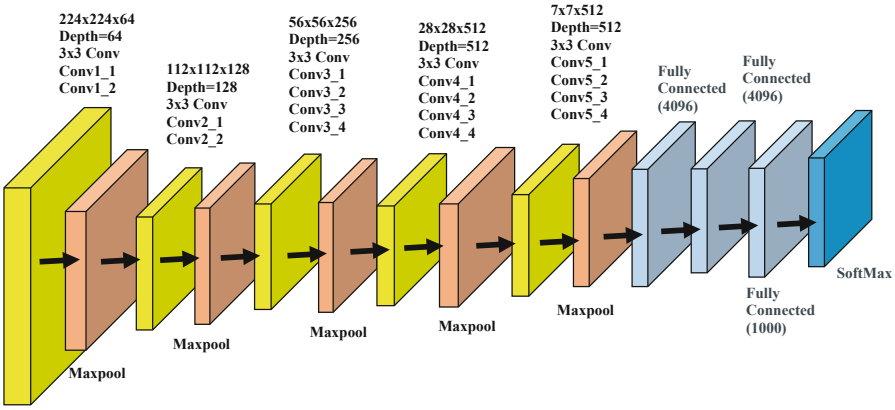

Fig. 2. The VGG-19 architecture

2.2 Lung Lesion Images Classification

This section clearly presents the proposed method for abnormal classifying. Chest X-ray images are valuable in detecting and diagnosing disease. Based on them, we can assess severity, respiratory complications, monitor treatment response and differential diagnosis. However, if only based on X-ray images, it is difficult to differentiate between viral pneumonia and some other etiologies. So, it must be combined with epidemiological characteristics and clinical manifestations to make a diagnosis. Suitable diagnosis. The types of lung lesions caused by Covid-19 that can be seen on X-ray images are: nodules, opacities, multifocal circular opacities, multifocal peripheral pulmonary parenchymal solidification.

Ground glass opacity is an incompletely solidified lesion with a higher density than the surrounding lung parenchyma, the border of blood vessels or bronchi inside the lesion can still be seen. Nodular opacities image are the opacities less than 3cm in diameter, round shape, may be scattered in the lung parenchyma. Pulmonary nodules are often well-demarcated, surrounded by lung parenchyma, and discontinuous with hilar or mediastinum. Bronchial wall thickening are lesions that show thickening of the bronchial wall, due to the accumulation of fluid or mucus around the bronchial wall, in the interstitial tissue. Thickened interlobular septum image associated with interlobular sulcus, cellular infiltration or fibrosis. In viral pneumonia, thickening of the septum is seen in diffuse lesions in acute respiratory distress syndrome.

In the early stages of the disease, X-ray images may be normal. Lesions are often both in the lung parenchyma and in the interstitium. Lesions are usually diffuse, bilateral

lower lobes, in the periphery and with little destruction. When the disease is cured, the lungs may become fibrous.

To classify lung lesion images, the proposed method presented as Fig. 3, includes the stages as: features extraction by U-net modify and VGG-19 combined on adaboost classification.

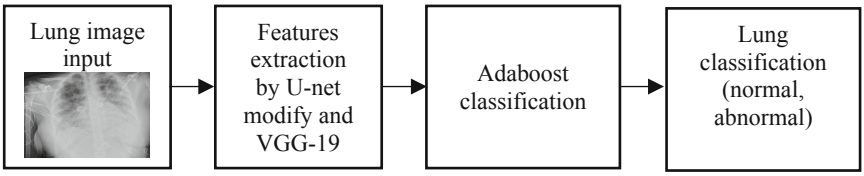

Fig. 3. The proposed method for lung classification

The parameters of MoU-Net presented as Fig. 1. The MoU-Net architecture with 5 pooling and 5 unpooling [15]. MoU-Net has the unpooling layer with kernels of size 2 × 2, stride 2 × 2 to get output consistent with the adaboost. So, the features filtering from the input image will be better than U-Net [15].

VGG-19 is a trained CNN. The number 19 is the number of layers with trainable weights including 16 convolutional layers and 3 fully connected layers. The parameters of VGG-19 presented as Fig. 2 and Table 1.

AdaBoost (Adaptive Boost) is a powerful learning algorithm that accelerates the generation of a strong classifier. It selects good features in a family of weak classifiers and recombines them linearly using weights. Therefore, it gradually improves accuracy by effectively applying a series of weak classifiers.

The adaboost algorithm maintains a normal distribution of weights on each training sample. In the first iteration, the algorithm training a weak classifier using a Haar-like feature performed best to detect the training samples. In the second iteration, the samples used for training, but misclassified by the first weak classifier, are given higher weights such that the Haar-like feature selected this time which must focus the computational ability for these misclassified test pieces. The process iterates and the end results are a cascade of linear combinations of weak classifiers, creating a strong classifier. Therefore, it helps to improve classification accuracy. The algorithm of adaboost as following [16]:

+ Given a set of n samples marked (x_1, y_1), (x_2, y_2),…., (x_n, y_n), where $x_k \in (x_{k1}, x_{k2},\ldots, x_{km})$ is the feature vector and $y_k \in (-1,1)$ is the label of the pattern (1 for object, −1 for background).

+ Initialize the initial weights for all samples, where m is the number of true samples (for object and $y = 1$) and l is the number of false samples (for background and $y = -1$)

$$W_{1,k} = \frac{1}{2m}, \frac{1}{2l} \tag{1}$$

+ Constructing T weak classifiers. Looping $t = 1,\ldots,$ T. For each feature in the feature vector, construct a weak classifier h_j with threshold θ_j and error ε_j:

$$\varepsilon_j = \sum_k^n W_{1,k} \left| h_j(x_k) - y_k \right| \tag{2}$$

Table 1. The parameters of VGG-19 combined on adaboost for classification

VGG-19 architecture	VGG-19 combined on Adaboost for classification
Conv3 × 3 (64) Conv3 × 3 (64)	Conv3 × 3 (64) Conv3 × 3 (64)
MaxPool	MaxPool
Conv3 × 3 (128) Conv3 × 3 (128)	Conv3 × 3 (128) Conv3 × 3 (128)
MaxPool	MaxPool
Conv3 × 3 (256) Conv3 × 3 (256) Conv3 × 3 (256) Conv3 × 3 (256)	Conv3 × 3 (256) Conv3 × 3 (256) Conv3 × 3 (256) Conv3 × 3 (256)
MaxPool	MaxPool
Conv3 × 3 (512) Conv3 × 3 (512) Conv3 × 3 (512) Conv3 × 3 (512)	Conv3 × 3 (512) Conv3 × 3 (512) Conv3 × 3 (512) Conv3 × 3 (512)
MaxPool	MaxPool
Conv3 × 3 (512) Conv3 × 3 (512) Conv3 × 3 (512) Conv3 × 3 (512)	Conv3 × 3 (512) Conv3 × 3 (512) Conv3 × 3 (512) Conv3 × 3 (512)
MaxPool	MaxPool
Fully connected (4096) Fully connected (4096) Fully connected (1000)	Classification by adaboost
SoftMax	
Lable of image	Lable of image

+ Choosing h_j with the smallest ε_j, we get h_t:
ht: X → {1, −1}, Update weights:

$$W_{t+1,k} = \frac{w_{t,k}}{z_t} x \begin{cases} e^{-\alpha_t}, h_t(x_k) = y_k \\ e^{\alpha_t}, h_t(x_k) \neq y_k \end{cases} \tag{3}$$

where,

$$\alpha_t = \frac{1}{2} ln(\frac{1-\varepsilon_j}{\varepsilon_j}) \tag{4}$$

Z_t is the coefficient that used to move W_{t+1} to the range [0, 1]. Strong classifier is built:

$$H(x) = sign(\sum_{t=1}^{T} \propto_t h_t(x)) \tag{5}$$

3 Experimental Results

Our experimental programs were developed by the python language on a computer of Intel core i7, 3.2 GHz CPU and 16 GB DDR3 memory. The lung images in the Covid-19 Radiography dataset [17] are used in our experiments. In this dataset, there are four categories such as: Covid, lung opacity, viral pneumonia, and normal chest X-ray images.

The total of images in this dataset are 21165 images, where 3616 Covid images, 6012 lung opacity images, 1345 viral pneumonia images and 10192 normal images. From the numbers of these images, we see that the numbers of images are not balanced in all above classes. Now, we select the number of images (sub-dataset) in this dataset to create a balanced dataset. In our experiments, we only use two sub-datasets with 1500 covid images and 1500 normal images.

The size of each image is 299 $\times$ 299 pixels resolution with Portable Network Graphics (.png) file format. We divided randomly the sub-dataset for 70% training and 30% testing. Some images in this sub-dataset are presented as Fig. 4.

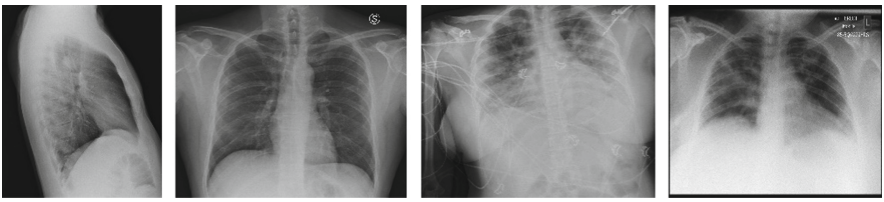

Fig. 4. Some images in sub-dataset

The accuracy is used to evaluate the metrics of the results classification. Sensitivity (Se) defines the ability to detect abnormal images and ranges from 0 to 1. The value of sensitivity range is calculated as Eq. (6).

$$Se = \frac{TP}{TP + FN} \tag{6}$$

where, TP is the number of true positives and FN is the number of false negatives. P and N are the total number of non-responsive and responsive samples in the dataset, respectively.

Specificity (Sp) defines the ability to distinguish images that have abnormal or not and ranges from 0 to 1. The value of specificity ranges is calculated as in the Eq. (7).

$$Sp = \frac{TN}{TN + FP} \tag{7}$$

where, TN is the number of true negatives, FP is the number of false positives.

Accuracy (Acc) represents the result accuracy of the proposed method in the test dataset, and ranges from 0 to 1 (equivalent in the range from 0% to 100%). The accuracy values are calculated as Eq. (8).

$$Acc = \frac{TP + TN}{TP + FN + TN + FP} \tag{8}$$

The experimentations are implemented with all the images in the above datasets. Table 2 presented the evaluation values of adaboost method and some deep learning models: U-Net, MoU-Net, VGG-16, VGG-19 and MoU-Net combined on VGG-19 for lung lesion images classification.

Table 2. The evaluation of the lung lesion images classification (%) between the adaboost and deep learning models.

Method	U-Net + adaboost method	MoU-Net + adaboost method	VGG-16 + adaboost method	VGG-19 + adaboost method	MoU-Net + VGG-19 + adaboost method
Accuracy (%)	93.721	95.582	92.167	93.123	97.598

In Table 2, we apply adaboost for classification. The result of combination of the MoU-Net and VGG-19, and adaboost method is better than others.

Table 3. The classification average evaluation between the proposed method with the recent methods.

Method	Year	The Covid-19 Radiography dataset		
		Sensitivity	Specificity	Accuracy
Vasilis method [18]	2021	0.9302	0.9512	0.9404
Cengil method [19]	2021	0.9574	0.9635	0.9604
Muhammad method [20]	2022	0.9631	0.9711	0.9671
Proposed method	2022	0.9710	0.9807	0.9761

Table 3 presents the results of the proposed method with the recent methods for classification. The average accuracy of the proposed method is 97.61% while the average accuracy of Vasilis method [18], Cengil method [19] and Muhammad method [20] are 94.04%, 96.04% and 96.71%, respectively.

As presented in Sect. 2.2, the MoU-Net architecture with more depth includes 5 pooling and 5 unpooling. The U-Net tradition architecture is only 4 pooling and 4 unpooling. Moreover, we also use VGG-19 and adaboost algorithms to improve the classification task. While Vasilis method [18] used a CNN and added a dense layer on top of a pre-trained baseline CNN (Efficient Net-B0), Cengil method [19] used the CNN architectures such as Alexnet, Xception, NASNETLarge, and Efficient Net-B0 are used as backbones to classify Covid-19 images. And Muhammad method [20] used a hybrid algorithm (Whale-Elephant Herding) for classification. It explains why the proposed method gives the better results versus the other methods.

4 Conclusions and Future Works

The main function of the lungs is to exchange gasses to maintain life, because the capillaries in the alveoli form a dense network. The lungs carry oxygen from the air into the pulmonary veins, and carbon dioxide from the pulmonary arteries out. The lungs are also involved in the metabolism and synthesis of many important substances, filter some toxins in the blood, and are also a place to store blood. Therefore, the factors affecting the lungs that will most damage the lungs are Covid-19. This paper proposed a method to improve U-Net and VGG-19 architectures combined on adaboost techniques for lung lesion images classification. The MoU-Net architecture with 5 pooling and 5 unpooling. MoU-Net has the unpooling layer with kernels of size 2×2, stride 2×2 to get output consistent with the adaboost. So, the features filtering from the input image will be better than U-Net. To evaluate the obtained results, we compare the results of the proposed method with other methods. Our experiment results are better than others in the Covid-19 Radiography dataset. To crease the accuracy of the proposed method, the improving VGG-19 architecture and the time running are necessary and experiment on other datasets in future work.

Acknowledgement. We acknowledge the support of time and facilities from Ho Chi Minh City University of Technology (HCMUT), VNU-HCM and University of Cuu Long for this study.

References

1. Nogrady, B.: What the data say about asymptomatic COVID infections, Nature **587** (7835), 534–535 (2020). https://www.nature.com/articles/d41586-020-03141-3. Accessed 16 May 2022
2. Hong, J.-M., et al.: Epidemiological characteristics and clinical features of patients infected with the COVID-19 virus in Nanchang, Jiangxi China. Front. Med. **7**(571069), 1–9 (2020). https://doi.org/10.3389/fmed.2020.571069
3. Bwire, G.M., Majigo, M.V., Njiro, B.J., Mawazo, A.: Detection profile of SARS-CoV-2 using RT-PCR in different types of clinical specimens: a systematic review and meta-analysis. J. Med. Virol. **2021**(93), 719–725 (2021). https://doi.org/10.1002/jmv.26349
4. Hu, Z., Tang, J., Wang, Z., Zhang, K., Zhang, L., Sun, Q.: Deep learning for image-based cancer detection and diagnosis-a survey. Pattern Recogn. **83**, 134–149 (2018)
5. Paweł, J., Dawid, S., Patryk, O.: Artificial intelligence for COVID-19 detection in medical imaging - diagnostic measures and wasting- a systematic umbrella review. J. Clin. Med. **11**, 1–16 (2022). https://doi.org/10.3390/jcm11072054
6. Chung, M., et al.: CT imaging features of 2019 novel coronavirus (2019-nCoV). Radiology **295**(1), 202–207 (2020)
7. Kroft, L.J.M., van der Velden, L., Girón, I.H., Roelofs, J.J.H., de Roos, A., Geleijns, J.: Added value of ultra–low-dose computed tomography, dose equivalent to chest X-ray radiography, for diagnosing chest pathology. J. Thorac. Imaging **34**(3), 179–186 (2019)
8. Li, L., et al.: Artificial intelligence distinguishes COVID-19 from community acquired pneumonia on chest CT. Radiology **296**(2), 65–71 (2020)
9. The, N.H., Nhung, N.T.H., Binh, N.T.: Adaptive lung diseases images classification technique based on deep learning. In: Van Toi, V., Nguyen, TH., Long, V.B., Huong, H.T.T. (eds.) 8th International Conference on the Development of Biomedical Engineering in Vietnam. BME

2020. IFMBE Proceedings, vol. 85, pp. 803-814. Springer, Cham (2021). https://doi.org/10.1007/978-3-030-75506-5_65
10. Javaheri, T., et al.: CovidCTNet: an open source deep learning approach to diagnose covid-19 using small cohort of CT images. NPJ. Digit. Med. **4**, 1–10 (2021)
11. https://www.kaggle.com/kmader/finding-lungs-in-ct-data. Accessed 16 May 2022
12. Kalane, P., Patil, S., Patil, B.P., Sharma, D.P.: Automatic detection of COVID-19 disease using U-Net architecture based fully convolutional network. Biomed. Sign. Process. Control **67**, 1–9 (2021). https://doi.org/10.1016/j.bspc.2021.102518
13. Hien, N.M., Binh, N.T., Viet, N.Q.: Edge detection based on fuzzy C means in medical image processing system. In: Proceedings of the IEEE International Conference on Systems Science and Engineering, pp. 12–15 (2017). https://doi.org/10.1109/ICSSE.2017.8030827
14. Hemdan, E.E.D., Shouman, M.A., Karar, M.E.: Covidx-net: a framework of deep learning classifiers to diagnose covid-19 in X-ray images, pp 1–4 (2020). arXiv:200311055
15. Binh, N.T., Hien, N.M., Tin, D.T.: Improving U-Net architecture and graph cuts optimization to classify arterioles and venules in retina fundus images. J. Intell. Fuzzy Syst. **42**(4), 4015–4026 (2022). https://doi.org/10.3233/JIFS-212259
16. http://www.robots.ox.ac.uk/~az/lectures/cv/adaboost_matas.pdf. Accessed 16 May 2022
17. https://www.kaggle.com/datasets/tawsifurrahman/covid19-radiography-database. Accessed 16 May 2022
18. Nikolaou, V., Massaro, S., Fakhimi, M., Stergioulas, L., Garn, W.: COVID-19 diagnosis from chest X-rays: developing a simple, fast, and accurate neural network. Health Inf. Sci. Syst. **9**(1), 1–11 (2021). https://doi.org/10.1007/s13755-021-00166-4
19. Cengil, E., Çınar, A.: The effect of deep feature concatenation in the classification problem: an approach on COVID-19 disease detection. Int. J. Imaging Syst. Technol. **32**(1), 26–40 (2021). https://doi.org/10.1002/ima.22659
20. Muhammad, A.K., et al.: COVID-19 classification from chest X-ray images: a framework of deep explainable artificial intelligence. Comput. Intell. Neurosci. 2022, 1–14 (2022). Article ID 4254631